

AD-A087 226

GEORGIA INST OF TECH ATLANTA CENTER FOR THE ADVANCEM--ETC F/6 20/11
DYNAMIC FRACTURE ANALYSIS: A TRANSLATING - SINGULARITY FINITE E--ETC(U)
JUN 80 S N ATLURI; Y NISHIOKA N00014-78-C-0636
GIT-CACH-SNA-22 NL

UNCLASSIFIED

| OF |
40
AD87226



END
DATE
FILMED
9-80
DTIC

LEVEL II

(1)
D.S.

Office of Naval Research

Contract ⁽¹⁵⁾ ~~NOO~~ 14-78-C-0636 NR 064-610

⁽⁹⁾ Technical Report No. 6

Report No. GIT-CACM-SNA-22, ⁽¹⁴⁾ T11-6

⁽⁶⁾ DYNAMIC FRACTURE ANALYSIS: A TRANSLATING - SINGULARITY
FINITE ELEMENT PROCEDURE

by

⁽¹⁰⁾ Satya N. Atluri and T. Nishioka

DTIC
ELECTRONIC
SERIALS
SECTION

11 JUN 80

12 10

Center for the Advancement of Computational Mechanics
School of Civil Engineering
Georgia Institute of Technology
Atlanta, Georgia 30332

This document has been approved
for public release and sale; its
distribution is unlimited.

80 7 24 039

411865

ADA 087226

DDC FILE COPY.

DYNAMIC FRACTURE ANALYSIS: A TRANSLATING - SINGULARITY
FINITE ELEMENT PROCEDURE.

S.N. Atluri, and T. Nishioka

Center for the Advancement of Computational Mechanics
School of Civil Engineering
Georgia Institute of Technology, Atlanta, Georgia 30332, USA.

ABSTRACT:

In this paper an efficient finite element method, which accounts for the translating singularities near the tip of a dynamically propagating crack, is presented. Two aspects of analyses of dynamic fracture, namely, (i) determination of dynamic stress-intensity factors from given crack velocity history, and (ii) determination of crack-velocity history (and arrest) from given dynamic-fracture-toughness versus crack-velocity data are considered. Results are presented and discussed for wedge-loaded rectangular, as well as tapered, double-centilever beam specimens.

KEYWORDS:

Dynamic Fracture, Propagating Crack Eigen Functions, Translating Singularities, Finite Elements, Dynamic Stress-intensity Factor, Dynamic Fracture Toughness, Prediction of Crack Propagation.

INTRODUCTION

A number of analytical and experimental investigations, into dynamic propagation and arrest of cracks in structural metals, have been conducted in recent years due, in part, to the important technical problems in assessing the structural integrity of flawed ship structures and of nuclear pressure vessels, and the need to develop criteria for crack arrest in these situations. Analytical solutions exist, for the most part, for boundary-value problems in linear elastodynamics for cracks in unbounded media. The problem of finite bodies, wherein the interaction of stress-waves reflected from the boundaries and/or the other crack-tip with the considered crack-tip, play an important role, is amenable for analysis, in most cases, only through numerical techniques. The literature on numerical methods, such as finite elements and finite differences, in dynamic fracture has been succinctly reviewed by Kanninen (1978). Most of the techniques reviewed by Kanninen (1978) fall into the category of "node-release techniques".

Recently, Atluri, Nishioka, and Nakagaki (1979), and Nishioka, and Atluri (1980 a,b,c) have presented formulations for a moving-singularity finite element method for simulating fast crack propagation in finite bodies. An energy-consistent variational statement is first developed (Atluri, Nishioka, and Nakagaki, 1979; Nishioka, and Atluri, 1980 a), as a basis for the above "moving singular-element" procedure of dynamic fracture analysis. The above numerical procedure has been applied (Nishioka and Atluri, 1980 b,c) in studying the finite-domain counterparts

of the problems with unbounded domains for which analytical solutions exist (Broberg, 1960; Baker, 1962; Nilsson, 1972; Freund, 1973). The obtained numerical results have been found to correlate excellently with the cited analytical solutions for infinite domains, during the time intervals for which these analytical solutions may be considered as valid. The computed solutions beyond these times, and the knowledge of the various time periods involved for wave-interaction in finite bodies, indicated both qualitatively as well as quantitatively the effects of stress-wave interactions on dynamic K-factors for cracks propagating in finite bodies.

In this paper, attention is primarily focused on the "application phase", viz., the determination of crack-tip velocity history (and possible crack arrest) from a given dynamic-fracture-toughness (K_{ID}) versus the crack-velocity ($\dot{\Sigma}$) relation, using the above described numerical procedure. To this end, the experimental results of Kalthoff, Beinert, and Winkler (1977, 1978) on wedge-loaded rectangular (WL-RDCB) as well as tapered (WL-TDCB) double cantilever beam specimens are considered. In the first-phase of the presently reported study, the experimental results for $\dot{\Sigma}$ versus time for the WL-RDCB specimen are simulated so as to numerically determine the dynamic K-factor variation with time and compare it with the reported experimental (caustics) measurements of dynamic K-factors. In the second phase of the study, using the reported (Kalthoff, Beinert, and Winkler, 1977; 1978) experimental results for K_{ID} versus $\dot{\Sigma}$ relations, and the crack-initiation stress-intensity factor K_{IQ} , the crack-propagation history in WL-RDCB, and WL-TDCB specimens is numerically predicted and compared with cited experimental results. The present results are also compared, where possible, with independent numerical results of Kobayashi (1979). Discussions are presented on the possible specimen-geometry dependence of the K_{ID} vs $\dot{\Sigma}$ relation.

OUTLINE OF TRANSLATING-SINGULARITY FINITE-ELEMENT METHOD

As derived by Atluri, Nishioka, and Nakagaki (1979), the virtual work equation applicable to a system of finite elements used to model the cracked body, between the times t_1 and t_2 , during which a Mode-I type crack-growth by an amount $\Delta\Sigma$ takes place can be written as:

$$\begin{aligned} & \frac{1}{n} \left[\int_{V_{Rn}} \{ (\underline{\sigma}^2 + \underline{\sigma}^1) : \delta \underline{\epsilon}^2 + \rho (\underline{u}^2 + \underline{u}^1) \cdot \delta \underline{u}^2 \} dv - \int_{S_{on}} (\underline{T}^2 + \underline{T}^1) \cdot \delta \underline{u}^2 ds \right. \\ & \left. - \int_{\Sigma_n^+} (\underline{T}^2 + \underline{T}^1) \cdot \delta \underline{u}^2 d\Sigma \right] + \int_V \{ (\underline{\sigma}^2 + \underline{\sigma}^1) : \delta \underline{\epsilon}^2 dv + \rho (\underline{u}^2 + \underline{u}^1) \cdot \delta \underline{u}^2 dv \} \\ & - \int_{\Sigma_n^+} (\underline{T}^2 + \underline{T}^1)^+ \cdot \delta \underline{u}^{2+} d\Sigma - \int_{\Delta\Sigma^+} (\underline{T}^2 + \underline{v}^1 \cdot \underline{\sigma}^1) \cdot \delta \underline{u}^{2+} ds = 0 \end{aligned} \quad (1)$$

In the above, V is the domain of the singularity-element; Σ is the crack-surface contained within the boundary of V at time t_1 ; the super-script (+) refers to the upper-half of the crack-surface which only is modelled in symmetric Mode-I case; $\Delta\Sigma$ is the amount of crack growth between times t_1 and t_2 ; V_{Rn} is the n^{th} regular (isoparametric) finite element in the cracked-body; S_{on} is that portion of the boundary (away from the crack) of V_{Rn} ; $\underline{\sigma}$, \underline{T} , \underline{u} , $\delta \underline{\epsilon}$, $\delta \underline{u}^{on}$ are, respectively, the stress tensor, applied traction vector, displacement vector, virtual strain tensor, and virtual displacement vector; the superscripts (1) and (2) denote, respectively the quantities at times t_1 and t_2 ; \underline{v}^1 is the unit normal vector to $\Delta\Sigma$. In the above the notation $\underline{\sigma} : \delta \underline{\epsilon} = \sigma_{ij} \delta \epsilon_{ij}$ and $\underline{T} \cdot \delta \underline{u} = T_i \delta u_i$ has been used. Note that at time t_2 , when the crack has opened by an additional amount $\Delta\Sigma$, the admissible virtual displacements are such that $\delta u_i^2 \neq 0$ at $\Delta\Sigma$.

In the present procedure, the displacement field within the singular-element, V_s , is assumed to be:

$$u_\alpha(\xi, x_2, t) = \sum_m^* u_{\alpha m}^*(\xi, x_2, v) \beta_m(t) + \text{Rigid body modes } (\alpha=1,2) \quad (2)$$

When $u_{\alpha m}^*$ are eigen-function solutions for the elastodynamic problem of steady-state (with respect to an observer moving with the crack-tip) crack-propagation at constant velocity v , as given in Atluri, Nishioka, and Nakagaki (1979). If x_1 (along the crack-axis) and x_2 (normal to crack-axis) are fixed cartesian coordinates, (ξ, x_2) is the coordinate system that moves with the crack-tip, i.e., $\xi = x_1 - vt$. In the present procedure, the assumed displacement field at times t_1 and t_2 , respectively, is taken to be that corresponding to Eq. (2) wherein the velocity v takes on the values v_1 and v_2 , viz., the velocities at times t_1 and t_2 . It is further seen from the properties of the above eigen-functions (Atluri, Nishioka, and Nakagaki, 1979) that $\beta_m(t)$ in Eq. (2) is in fact the dynamic stress-intensity factor and hence may be computed directly.

The total velocity and acceleration of a material particle in V_s are then:

$$\dot{u}_\alpha = \sum_m^* u_{\alpha m}^* \dot{\beta}_m - v \sum_m^* u_{\alpha m, \xi}^* \dot{\beta}_m \quad (3)$$

$$\text{and } \ddot{u}_\alpha = \sum_m^* u_{\alpha m}^* \ddot{\beta}_m - 2v \sum_m^* u_{\alpha m, \xi}^* \dot{\beta}_m + v^2 \sum_m^* u_{\alpha m, \xi\xi}^* \beta_m \quad (4)$$

where $(\cdot)_{,\xi} = \partial(\cdot)/\partial\xi$. The compatibility of displacement, velocity, and acceleration at the boundary of V_s with the surrounding regular elements is satisfied through a least-squares technique (Atluri, Nishioka, and Nakagaki, 1979).

Assuming that, between times t_1 and t_2 , crack growth occurs (which can be determined, as explained below, in the so-called "application phase" calculations using the given material characteristic of a K_{ID} versus $\dot{\Sigma}$ relation; or is known a priori, in the so-called "generation phase" calculation, i.e., in the case of simulation of given $\dot{\Sigma}$ versus time data), the singularity element is translated, by an appropriate distance $\Delta\Sigma$ from its location at time t_1 as shown in Fig. 1.

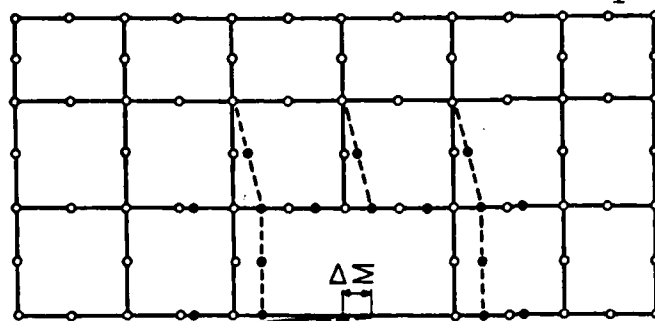


FIGURE 1

Crack
 • Old nodal points ($t=t_1$)
 • New nodal points ($t=t_2$)

ACQUISITION FOR	<input checked="" type="checkbox"/>			
DTIC GR&I				
DTIC TAB				
Unannounced				
Justification				
By				
Distribution/				
Availability Codes				
Available/for				
Special				
Dist	A			

Note that, unlike in the node-release technique of Kobayashi (1979), the above shown amount $\Delta\Sigma$ is not, in any way, related to the distance between any two adjacent finite element nodes at time t_1 . Note also from Fig. 1 that, as the singular-element is translated, the surrounding regular elements are appropriately distorted. After a sufficient amount of translation, say $M(\Delta\Sigma)$, of the singular-element, the distortion of the regular-elements may become acute. In such a case, the regular finite element mesh is readjusted, as described in Nishioka, and Atluri (1980a).

The finite element equation obtained by using the variational principle of Eq.

(1) can be shown to be:

$$\begin{aligned} \ddot{m} \ddot{q}_2 + K q_2 &= \bar{Q}_2 + \bar{Q}_1 - K q_1 - m \ddot{q}_1 \text{ for } V_R \\ m \ddot{q}_{s2} + D \dot{q}_{s2} + K_s q_{s2} &= Q_s \text{ for } V_s \end{aligned} \quad (4)$$

where V_R is the region spanned by regular elements. It is shown by Nishioka and Atluri (1980a) that out of all the matrices appearing in Eq. (4), two, viz., K and D are unsymmetric, due to the use of the eigen-functions in the moving coordinate system (ξ, x_s) as in V_s . The Eqs. (4) are numerically solved in the present, using the well-known Newmark- β method. Once the displacements, velocities, and accelerations (viz., q_{s2} , \dot{q}_{s2} , and \ddot{q}_{s2}) at the nodes of V_s are solved for from Eq. (4), the undetermined parameters β_m , $\dot{\beta}_m$, and $\ddot{\beta}_m$ (and hence the dynamic stress-intensity factor, and its first and second time-derivatives) can be computed directly.

CALCULATION OF $K_I(t)$ FROM GIVEN $\dot{\Sigma}(t)$ DATA ("GENERATION PHASE"):

Since the crack-velocity $v = \dot{\Sigma}(t)$, is known, using the velocities v_1 and v_2 at times t_1 and t_2 , respectively, the finite element equations (4) can be easily constructed. From these, as explained above, β_1 (which is in fact equal to K_I), $\dot{\beta}_1$, and $\ddot{\beta}_1$ can be directly computed at time t_2 as well as at all subsequent times.

PREDICTION OF $\Sigma(t)$ FROM GIVEN K_{ID} VERSUS $\dot{\Sigma}(t)$ RELATION ("APPLICATION PHASE"):

Let the solution upto time t_1 be assumed to be known. In order to find the solution at t_2 from Eq. (4), the crack-velocity at t_2 , ie., $v_2 = \dot{\Sigma}(t_2)$ must be found. To this end, it is first noted that the dynamic stress-intensity factor can be written as:

$$K_I = K_I(t, v). \quad (5)$$

Since, in the present procedure, the velocity of crack-propagation is assumed to be constant within each time-step, an approximate procedure to predict the velocity at $[t_1 + (\Delta t/2)]$ will be sought. Using double Taylor series expansion, it is seen from Eq. (5) that:

$$K_{Ip}(t_1 + \frac{\Delta t}{2}; v_1 + \Delta v) = \sum_{n=0}^{\infty} \frac{1}{n!} \left\{ \left(\frac{\Delta t}{2} \right) \frac{\partial}{\partial t} + \Delta v \frac{\partial}{\partial v} \right\}^n K_I(t_1, v_1) \quad (6)$$

where K_{Ip} is the predicted K_I at $t_1 + (\Delta t/2)$ while $K_I(t_1, v_1)$ is known. One can now rewrite Eqn. (6) as:

$$\begin{aligned} K_{Ip} &= K_I(t_1, v_1) + \left(\frac{\Delta t}{2} \right) \dot{K}_I(t_1, v_1) + \frac{(\Delta t)^2}{8} \ddot{K}_I(t_1, v_1) + R \\ &\equiv \beta_1(t_1) + \left(\frac{\Delta t}{2} \right) \dot{\beta}_1(t_1) + \frac{(\Delta t)^2}{8} \ddot{\beta}_1(t_1) + R \equiv K_{Ip}^* + R \end{aligned} \quad (7a, b)$$

where, $(\dot{\quad}) = \partial(\quad)/\partial t$, R is the "residue" (all the omitted terms from the right-hand side of Eq. (6)), and as explained above, in the present procedure, $K_I(t_1) \equiv \beta_1(t_1)$, etc.

Using the predicted K_{Ip} of Eq. (7), and the given K_{ID} versus $\dot{\Sigma}(t)$ relation, the crack-velocity v (or $\dot{\Sigma}$) at time $[t_1 + (\Delta t/2)]$ can be predicted. Using this crack-velocity value, the finite element system of equation (4) at time t_2 can be constructed, and from these, the actual dynamic stress-intensity factor $K_I(t_2)$ can be computed. Thus, the actual K_I at $t_1 + (\Delta t/2)$ can be computed, as:

$$K_I(t_1 + \frac{\Delta t}{2}) \approx (1/2)[K_I(t_1) + K_I(t_2)] \quad (8)$$

The correlation between the predicted K_{Ip} of Eq. (7) and the actual K_I of Eq. (8) can be seen to depend on the residue ' R_{Ip} ' of Eq. (7). To ensure this correlation, a further approximation is introduced in the present work that the residue R at time $t_1 + (\Delta t/2)$ can be approximated by its known value at $t_1 - (\Delta t/2)$, in the generic case. Thus, in the present procedure, Eq. (7) is re-approximated as:

$$K_{Ip}(t + \frac{\Delta t}{2}) = \beta_1(t_1) + (\frac{\Delta t}{2})^2 \ddot{\beta}_1(t_1) + \frac{(\Delta t)^2}{8} \beta_1(t_1) - [K_I(t_1 - \frac{\Delta t}{2}) - K_{Ip}^*(t_1 - \frac{\Delta t}{2})] \quad (9)$$

In the present calculation, when Eqn. (7) with $R=0$ was used an error of the order of 3% between K_{Ip} and K_I was noted. However, when Eq. (9) was used, this error reduced to the order of 0.5%. Further algorithmic details of the prediction phase along with detailed error analysis studies, which are omitted here, will be reported elsewhere.

RESULTS OF GENERATION CALCULATIONS:

The presently used finite element mesh for the upper half of WL-RDCB specimen (Kalthoff and colleagues, 1977) is shown in Fig. 2. Note that, in the present translating singular-element procedure, this mesh represents the configuration at the beginning of the crack-propagation. The singular-element is shown by the shaded area in Fig. 2. Plane-strain conditions are invoked. The experimentally measured crack-length versus time history (as well as the crack-velocity versus time history) for the WL-RDCB specimen (reported by Kalthoff, Beinert, and Winkler, 1977) with a crack-initiation stress-intensity factor K_{Iq} (larger than fracture toughness K_{IC}) of $2.32 \text{ MN/m}^{3/2}$ are shown in Fig. 3.

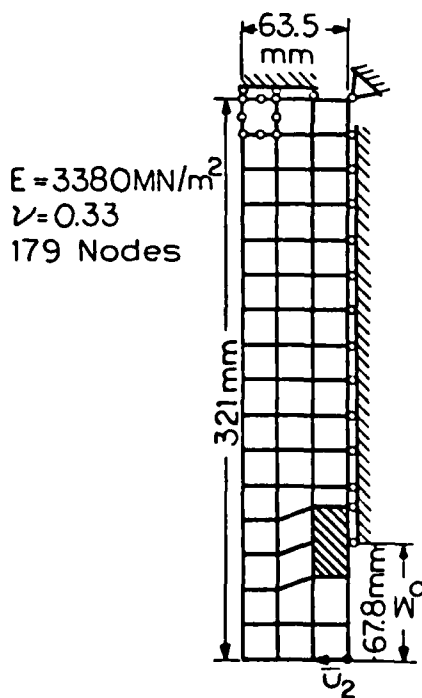


FIGURE 2

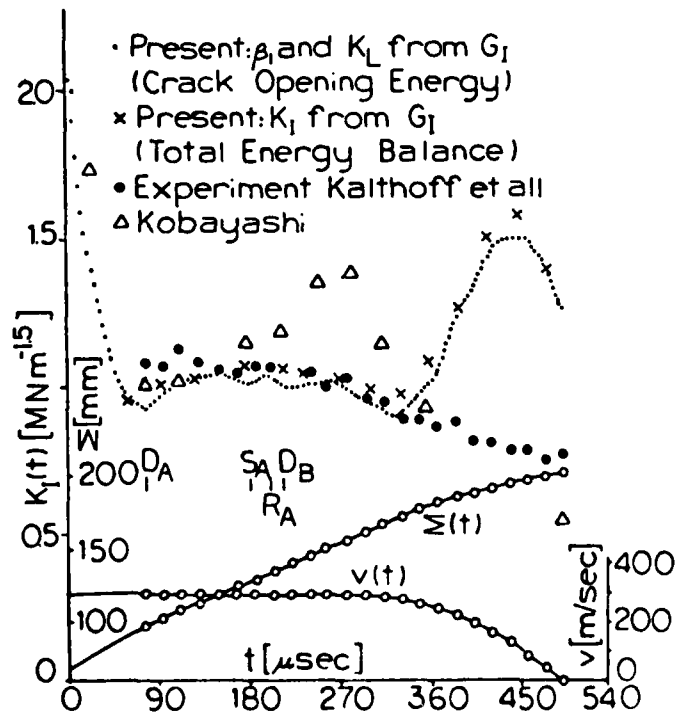


FIGURE 3

Also shown in Fig. 3 are: (i) the presently calculated dynamic K-factor, based on (a) direct evaluation of β_1 as explained earlier, (b) using the crack-opening energy as computed from the present variational formulation, and the crack-tip integral, and (c) using the crack-opening energy as computed from a global

energy balance, and (ii) the experimentally determined dynamic K-factors and (iii) the numerical results of Kobayashi [1979]. It is seen that the present results under (i)a and b are almost identical. It is also seen that the present results correlate excellently with those of Kalthoff and co-workers (1977) during the first (2/3) of the propagation history. However, during the last of (1/3) of propagation history, the present results exhibit a pronounced peak as compared to the experimental results. It is felt that this may be partly due to the fact that the present is a linear elastodynamic analysis while the experimental material (Araldite B) is viscoelastic in nature. It is interesting to note that the numerical results of Kobayashi (1979) also exhibit a pronounced peak as in the present results, except that this occurs much earlier in Kobayashi's results. The problem was reanalysed by slightly perturbing the data for $\dot{\Sigma}(t)$ curve. These results (not presented here for want of space) indicate that these slight perturbations, while not affecting the K-factor solution during the first (2/3) of propagation, do alter the magnitude of the above mentioned peak in the latter (1/3) of propagation. These results indicate the need for the extreme care with which experimental data for $\Sigma(t)$ should be recorded.

Results of Application Phase:

The experimental (Kalthoff and co-workers, 1977; 1978) results for K_{ID} versus $\dot{\Sigma}$ relation, for WL-RDCB and WL-TDCB specimens, that are used in the present analyses are shown in Fig. 4.

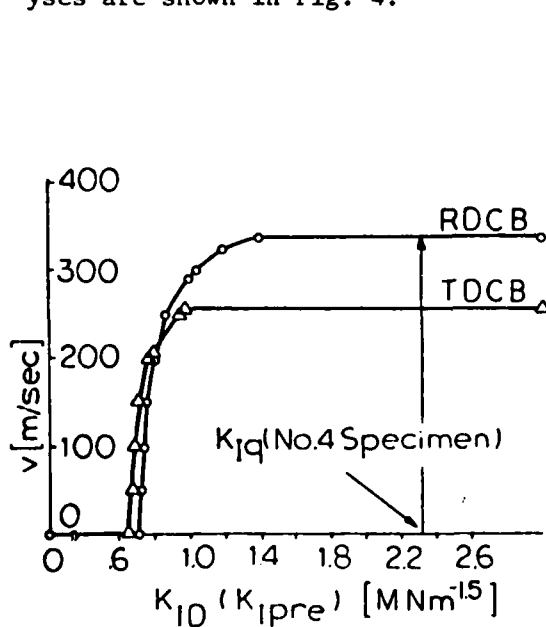


FIGURE 4

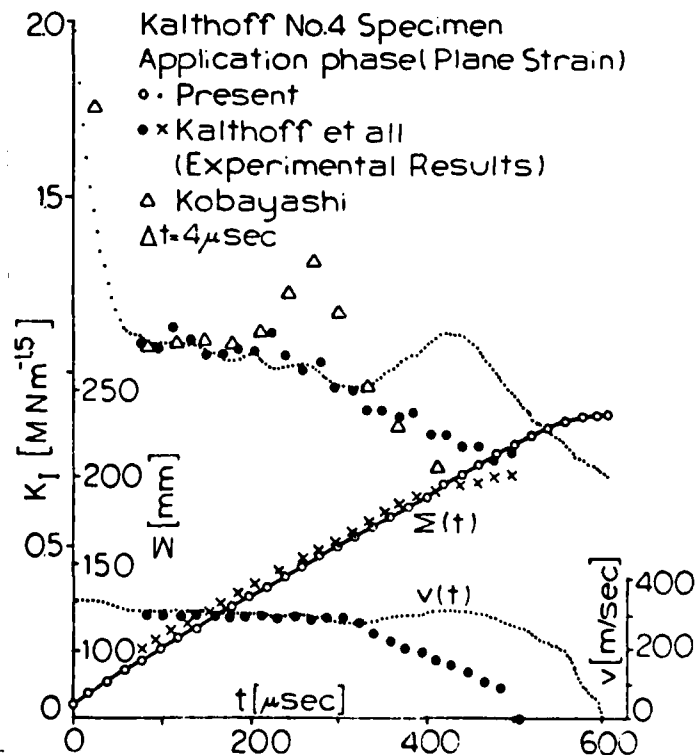


FIGURE 5

Two RDCB specimens, with K_{I0} values of 2.32 and 1.33 $\text{MN/m}^{3/2}$, respectively, were analyzed using a plane-strain assumption. Using the K_{ID} versus $\dot{\Sigma}$ relation of Fig. 4, the propagation histories in both specimens were predicted, using the earlier described procedure. The results for the two RDCB specimens are shown in Figs. 5 and 6 representively, along with comparison experimental results of Kalthoff and co-workers (1977) and available numerical results of Kobayashi (1979). It is seen that the present predictions agree excellently with the cited experimental

results. However, it is seen that, for the RDCB specimen with $K_{I0} = 1.33 \text{ MN/m}^{3/2}$, the predicted crack arrest length is about 19% higher than the experimental length. Once again, it is believed that this discrepancy is due to the inadequacy of the present linear-elastic material modeling. The variation of different energy quantities of interest during this predicted crack-propagation history, in the first RDCB specimen ($K_{I0} = 1.33 \text{ MN/m}^{3/2}$) is shown in Fig. 7. Since each of the indicated quantities T, U, and F, were calculated independently using the present procedures, the fact that their sum correlates excellently with the input energy W lends credence to the present calculations.

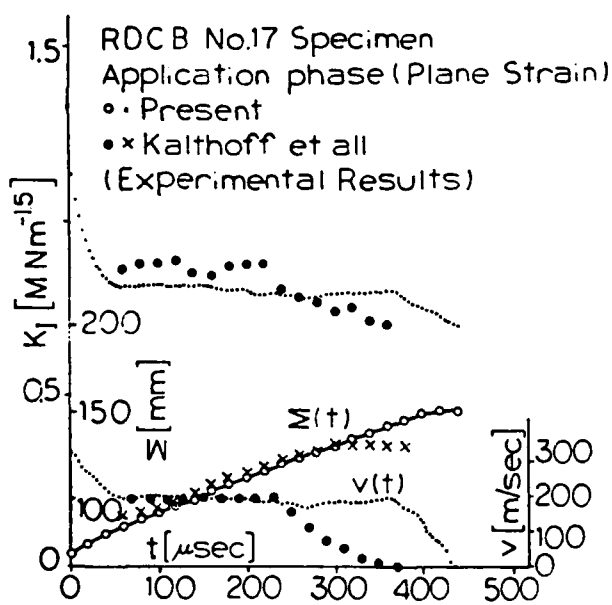


FIGURE 6

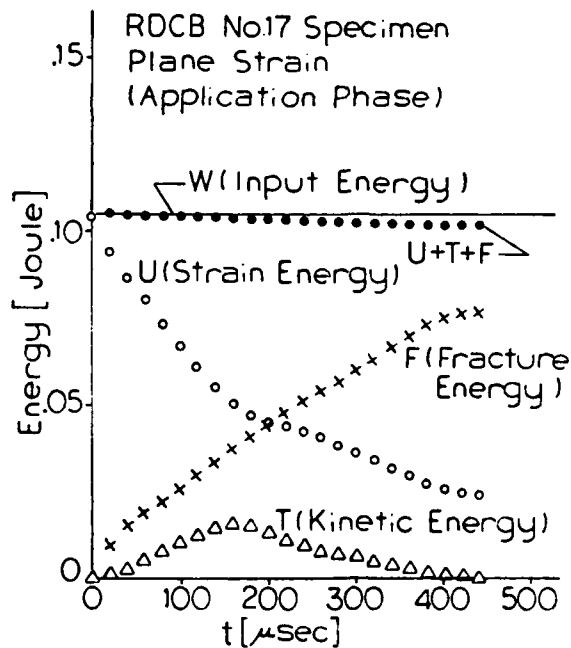


FIGURE 7

The finite element model for TDCB specimen (at initiation of propagation) is shown in Fig. 8. A K_{I0} value of $2.08 \text{ MN/m}^{3/2}$ is used. The predicted crack-propagation history, based on the K_{ID} vs $\dot{\epsilon}$ relation of Fig. 4, is shown in Fig. 9. Once again good correlation of the present results with the experimental ones (Kalthoff and co-workers, 1978) is noted.

Results were also obtained in a study of the possible specimen dependency of the K_{ID} versus $\dot{\epsilon}$ relation. These results, along with details of prediction phase calculations for several other specimens, which are omitted here for space reasons, are mentioned in the oral presentation of this paper and will be documented elsewhere.

Acknowledgement: This work has been supported by the U.S. Office of Naval Research under Contract N00014-78-0636. The encouragement of Dr. N. Perrone is greatly appreciated. Thanks are due to Ms. Peggy Eiteman for the care in typing this manuscript.

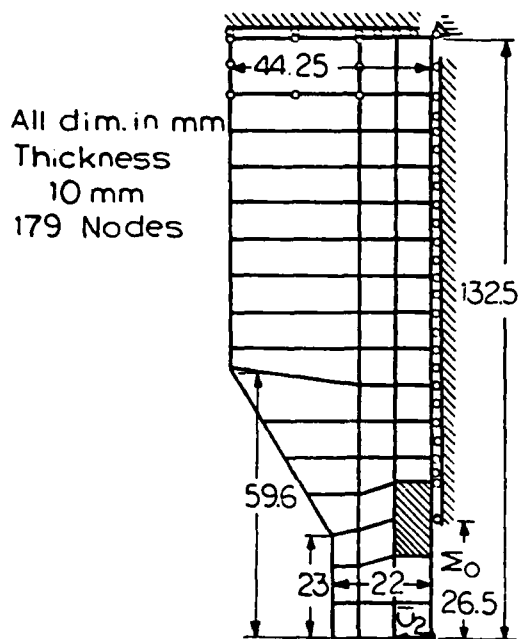


FIGURE 8

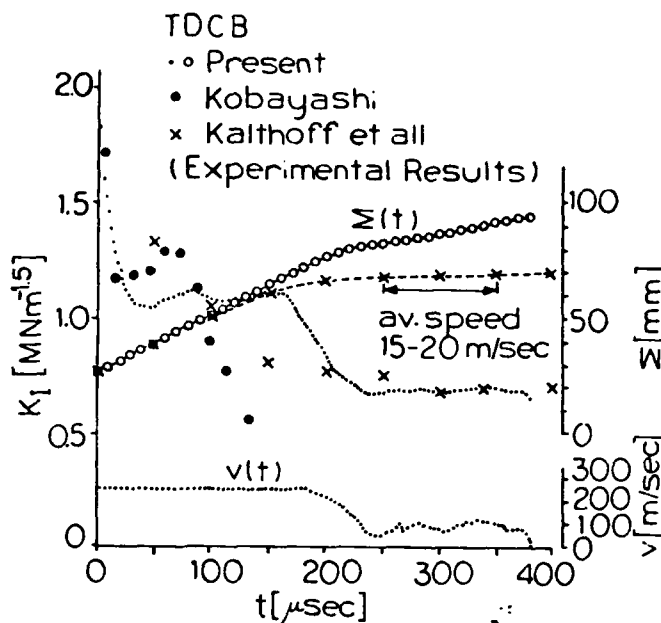


FIGURE 9

References:

- [1] Atluri, S.N., Nishioka, T., and Nakagaki, M., (1979) In N. Perrone, and S.N. Atluri, Eds. Nonlinear and Dynamic Fracture Mechanics ASME-AMD vol 35, ASME, N.Y., pp 37-67.
- [2] Baker, B.R. (1972) Jnl of Applied Mechanics ASME, 29 pp 449-545.
- [3] Broberg, K.B. (1960) Arkiv För Fysik 18, 10, pp 159-162.
- [4] Freund, L.B. (1973) Jnl of Mech Phys Solids 21, pp 47-61.
- [5] Kalthoff, J.F., Beinert, J., and Winkler, S., (1977), In G.T. Hahn, and M.F. Kanninen (Eds) Fast Fracture and Crack Arrest ASTM STP 627, pp 161-176.
- [6] Kalthoff, J.F., Beinert, J., and Winkler, S. (1978) In Proc. ASTM Symp. on Crack Arrest Methodology and Applications, Philadelphia Nov. 6-7, 1978.
- [7] Kanninen, M.F. (1978) In A.R. Luxmoore and D.R.J. Owen (Eds) Numerical Methods in Fracture Mechanics, University College, Swansea, pp 612-634.
- [8] Kobayashi, A.S. (1979) In N. Perrone, and S.N. Atluri (Eds) Nonlinear and Dynamic Fracture Mechanics ASME-AMD vol 35, ASME, N.Y., pp 19-35.
- [9] Nilsson, F. (1972) Internl Jnl Fracture 8, 4, pp 403-411.
- [10] Nishioka, T., and Atluri, S.N., (1980a) Journal of Applied Mechanics, ASME, Accepted for Publication.
- [11] Nishioka, T., and Atluri, S.N., (1980b) Journal of Applied Mechanics, ASME, Accepted for Publication.
- [12] Nishioka, T., and Atluri, S.N., (1980c) "Efficient Computational Techniques for the Analysis of Some Problems of Fracture in Pressure Vessels and Piping", Paper to be presented at ASME Pressure Vessel and Piping Conference, San Francisco, Aug. 1980.

REPORT DOCUMENTATION PAGE		READ INSTRUCTIONS BEFORE COMPLETING FORM
1. REPORT NUMBER GIT-CACM-SNA-22	2. GOVT ACCESSION NO. AD-A087 226	3. RECIPIENT'S CATALOG NUMBER
4. TITLE (and Subtitle) Dynamic Fracture Analysis: A Translating - Singularity Finite Element Procedure		5. TYPE OF REPORT & PERIOD COVERED Interim Report
7. AUTHOR(s) S.N. Atluri, and T. Nishioka		6. PERFORMING ORG. REPORT NUMBER GIT-CACM-SNA-22 ✓
9. PERFORMING ORGANIZATION NAME AND ADDRESS Center for the Advancement of Computational Mechanics School of Civil Engineering ✓ Georgia Institute of Technology, Atlanta, GA 30332		8. CONTRACT OR GRANT NUMBER(s) N00014-78-C-0636 ✓
11. CONTROLLING OFFICE NAME AND ADDRESS Office of Naval Research Structural Mechanics Program Dept. of the Navy, Arlington, VA 22217		10. PROGRAM ELEMENT, PROJECT, TASK AREA & WORK UNIT NUMBERS NR 064-610
14. MONITORING AGENCY NAME & ADDRESS (if different from Controlling Office)		12. REPORT DATE June 1980
		13. NUMBER OF PAGES 8
		15. SECURITY CLASS. (of this report) Unclassified
16. DISTRIBUTION STATEMENT (of this Report) Unlimited		15a. DECLASSIFICATION/DOWNGRADING SCHEDULE
<div style="border: 1px solid black; padding: 5px; display: inline-block;"> This document has been approved for public release and sale; its distribution is unlimited. </div>		
17. DISTRIBUTION STATEMENT (of the abstract entered in Block 20, if different from Report)		
18. SUPPLEMENTARY NOTES to appear in Proc. 5th Int. Conf. on Fracture (ICFS), Cannes, France, March 28-April 1, 1981		
19. KEY WORDS (Continue on reverse side if necessary and identify by block number) Dynamic Fracture, Propagating Crack Eigen Functions, Translating Singularities, Finite Elements, Dynamic Stress-intensity Factor, Dynamic Fracture Toughness, Prediction of Crank Propagation		
20. ABSTRACT (Continue on reverse side if necessary and identify by block number) In this paper an efficient finite element method, which accounts for the translating singularities near the tip of a dynamically propagating crack, is presented. Two aspects of analyses of dynamic fracture, namely, (i) determination of dynamic stress-intensity factors from given crack velocity history, and (ii) determination of crack-velocity history (and arrest) from given dynamic-fracture-toughness versus crack-velocity data are considered. Results are presented and discussed for wedge-loaded rectangular, as well as tapered, double-centilever beam specimens.		